Open access • Journal Article • DOI:10.1109/TNS.1979.4330082

Linac Particle Tracing Simulations — Source link

W. P. Lysenko

Institutions: Los Alamos National Laboratory

Published on: 01 Jan 1979 - IEEE Transactions on Nuclear Science (IEEE)

Topics: Accelerator physics, Beam emittance, Linear particle accelerator, Particle accelerator and Thermal emittance

LA-UR-79-709

conf. 790307--39

TITLE: LINAC PARTICLE TRACING SIMULATIONS

MASTER

AUTHOR(S): Walter P. Lysenko

SUBMITTED TO: Particle Accelerator Conference,
San Francisco, CA, March 12-14, 1979

University of California

LOS ALAMOS SCIENTIFIC LABORATORY
Post Office Box 1663 Los Alamos, New Mexico 87545
An Affirmative Action/Equal Opportunity Employer

LINAC PARTICLE TRACING SIMULATIONS*

Walter P. Lysenko
Los Alamos Scientific Laboratory, Los Alamos, NM 87545

Abstract

A particle tracing code was developed to study space-charge effects in proton or heavy-ion linear accelerators. The purpose is to study space-charge phenomena as directly as possible without the complications of many accelerator details. Thus, the accelerator is represented simply by harmonic oscillator or impulse restoring forces. Variable parameters as well as mismatched phase-space distributions were studied. This study represents the initial search for those features of the accelerator or of the phase-space distribution that lead to emittance growth.

Input Distributions and Matching[1]

In the absence of space charge, a two-dimensional phase-space distribution is matched if it has the same shape as that of the trajectories of the outer-most particles. With space charge, if forces do not depend explicitly on time, it is possible to produce six-dimensional phase-space distributions, called equilibrium distributions, that are time independent and are matched to the accelerator, even if space charge introduces nonlinearities and couplings.

Equilibrium calculations give space-charge limits in terms of accelerator parameters that are useful scaling laws for space-charge dominated beams. Because the single-particle Hamiltonian is conserved, we have equilibrium if the distribution function is a function of the Hamiltonian.

$$f(\vec{x},\vec{p}) = F(H) \quad . \qquad (1)$$

For the function F, we choose one of the following

$$F = \text{const.} \times n(H_0 - H)^{n-1} \quad , \qquad (2)$$

where n is an integer. These are the same functions used in the original one-degree-of-freedom work by Gluckstern, Chasman, and Crandall.[2] We generally consider n = 2 type distributions because they seem to correspond most closely to experimentally observed distributions.

We use the following two-degree-of-freedom model

$$H = \frac{p^2}{2m} + \frac{kr^2}{2} + \frac{k_z z^2}{2} + e\phi(r,z) \quad , \qquad (3)$$

where $\phi(r,z)$ is the unknown space-charge potential. All coordinates and momenta are relative to the synchronous particle. To determine ϕ we must solve a nonlinear Poisson equation with three parameters: μ, α, and n. The space-charge parameter μ is proportional to the particle density at the bunch center and is defined by

$$\mu = \frac{2k\mu_r + k_z\mu_z}{2k + k_z} \quad , \qquad (4)$$

where $-\mu_r$ is the ratio of the radial space-charge force to the radial external restoring force at the bunch center with a similar definition for μ_z. The tune depression factor in the direction i is $(1 - \mu_i)^{1/2}$. The parameter α is the ratio of the longitudinal force constant to the radial force constant and is the only accelerator parameter relevant to the space-charge physics in the present model.

The computer code RZED (R-Z Equilibrium Distribution) was written to solve the nonlinear Poisson equation. From the resulting distribution function, a relation between the beam current, emittance, and radius may be determined in terms of accelerator parameters (see Ref. 1).

$$I = F(\mu,\alpha,n)\,\frac{m}{e}\left(\mu^o_{shr}\right)^{1/2}(\eta f)^{3/2} \qquad (5a)$$

$$\frac{r}{\beta\lambda} = G(\mu,\alpha,n)\left(\frac{\eta f}{\mu^o_{shr}}\right)^{1/2}\beta^{-1} \quad , \qquad (5b)$$

TABLE I

ACCELERATOR PARAMETERS

Frequency	f	10^9 Hz
Initial velocity	β	0.04
Phase advance	μ^o_{shr}	27.4° (5T solenoid or B_{pole} = 1.5T quadrupole)
Electric field	E_0T	1.53 MV/m
Synchronous phase	ϕ_s	-30°

The space-charge physics calculated by RZED is contained in the functions $F(\mu,\alpha,n)$ and $G(\mu,\alpha,n)$. These space-charge effects are shown in Fig. 1 where the current and the radius are plotted as a function of the space-charge parameter. The other RZED parameters are fixed at $\alpha = 0.67$ and $n = 2$. These curves represent different equilibria for a fixed normalized transverse emittance value of $\eta = 7.4 \times 10^{-7}$ m-rad and for a fixed accelerator described by the parameters in Table I.

Higher density distributions correspond to larger beam radii. For a given accelerator, there is no limit to the current that can be transported except that the matched radius also increases without limit. To decrease the space charge effects (decrease μ) for a fixed current and emittance, one must decrease the beam radius by increasing the external focusing forces.

Variable Parameters

If the product $E_0T \sin\phi_s$ is proportional to β during acceleration, then the longitudinal focusing force is constant, and the bunch length remains fixed. This result holds for an equilibrium distribution even in the presence of space charge.

If the electric field and the synchronous phase remain constant, then, in the absence of space charge, the bunch length increases as $\beta^{1/4}$. With space charge this result is modified. It is important that the bunch length does not increase faster than β; if it does, the phase extent of the bunch will increase and will cause unstable longitudinal motion in a real accelerator with a finite potential well.

For slowly varying parameters we expect instantaneous equilibrium to be maintained, even though the condition given by Eq. (1) will not be preserved. (However, for one degree of freedom, Eq. (1) is preserved but the final F differs from the initial F.)

The HOT Code

The HOT (Harmonic Oscillator Tracing) code in its usual form uses harmonic oscillator restoring forces in all three directions. Acceleration is applied continuously. Couplings and nonlinearities occur only through space charge. The space charge forces are calculated with an area-weighted particle-in-cell method using a variable r-z mesh (up to 15 x 30 cells). Up to ten thousand macroparticles can be traced. Input tables provide the desired variation of transverse wavelengths, accelerating gradient, and synchronous phase as functions of the distance along the structure. Time is the independent variable.

*Work performed under the auspices of the U.S. Department of Energy.

TABLE II

TRANSVERSE SIZES AND EMITTANCES FOR MISMATCHED BEAMS

η/η_o	Initial Size[a] (mm)	Initial Emittance[b] (mm-mrad)	Final Size[a] (mm)	Final Emittance[b] (mm-mrad)
1	0.66	0.046	(matched)	
1/2	0.47	0.023	0.79	0.024
1/4	0.33	0.011	1.00	0.013
1/8	0.23	0.006	1.26	0.009

[a]Size of fitted transverse phase-space ellipse containing 90% of the particles.
[b]Normalized rms transverse emittance.

Simulations with Harmonic Longitudinal Potential

Slowly Varying Parameters. As an example, an accelerator with fixed transverse forces and with fixed values for the electric accelerating field and for synchronous phase was considered. A $\mu = 0.95$ initial distribution was used (such high-μ distributions cannot be accurately prepared but it turns out that small mismatches are not important). In accelerating from $\beta = 0.04$ to $\beta = 0.11$, the 90% and rms emittances in the three directions separately were conserved to within 3% and their sums were conserved to within 0.5%. Figure 2 shows the initial and final two-dimensional phase-space projections. The bunch length is shown as a function of velocity in Fig. 3. Note that the bunch length grows faster than $\beta^{1/4}$, which is the adiabatic no-space-charge result, but slower than β, so that phase damping is present.

Because the longitudinal restoring force decreases with β, the bunch length increases. This increase causes the net transverse focusing forces to increase. In our example, the final charge density is 0.7 of the initial value. The harmonic oscillator adiabatic invariant predicts a final beam radius of about 0.6 of the initial value. But we find in reality that the final radius is about 0.9 of the initial value so this space-charge coupling effect is small. At least part of the explanation is that the final distribution is more sharply peaked in the center than the initial distribution.

Mismatches. Linac simulations by Chesman[3] have indicated that the output emittance approaches a nonzero limit as the input emittance is reduced to zero. In the present model, Eq. (5) and Fig. 1 show that we can maintain equilibrium and still decrease the emittance indefinitely keeping the beam current and accelerator parameters fixed. In so doing, the space-charge parameter μ approaches unity and the matched beam radius increases indefinitely. There is no lower limit to the output emittance. Of course, the finite bore dimension will imposes a limit but there is no limit caused by emittance growth. Consider the situation where the x to x' ratio in a distribution is fixed and the emittance is reduced below its matched value keeping the current and accelerator parameters fixed. Starting with a $\mu = 0.95$ distribution with current I_o and emittance η_o, the current I required to maintain a match with a new emittance η can be obtained from the scaling law Eq. (5a)

$$I/I_o = (\eta/\eta_o)^{3/2} \quad . \tag{6}$$

Calculating a new lower current distribution produces a distribution with the desired smaller emittance η. But in the particle tracing simulation we let each macroparticle carry a charge corresponding to the original current I_o. The results are shown for a few cases in Table II.

For the mismatched cases, the radius grows quickly then fluctuates with twice the external frequency. Because the average beam radius is large, the average space charge forces are small so that the time to reach a maximum in the radius is about one-fourth the undepressed transverse period. It does not pay to decrease the beam radius to below its matched value because space-charge growth will only increase the radius to above its matched value.

The emittance growth is small so that a lower limit to the emittance, if it exists, will be very small (remember the beam is already near the space-charge limit even before the emittance is reduced). Because of the mismatch the phase-space area swept out by the beam is large and in the presence of external nonlinearities gives an effective emittance growth because of filamentation.

Discrete Gap Simulations

The above calculations used a continuous acceleration model with harmonic longitudinal restoring forces. Another version of BOT was used to determine if localizing the longitudinal forces to the gaps modifies the results. Whenever a particle crosses a gap, it receives an energy increase equal to $eE_oT \cos \phi$, where ϕ is the rf phase at the time of gap crossing. At the time the synchronous particle crosses the gap, all particles are given another energy change because of the new reference energy. Besides making the acceleration and longitudinal focusing discrete, this procedure also makes the effective longitudinal potential nonlinear.

In using the nonlinear potential a new problem arises when space charge is included because the size of the finite potential well is reduced.* To longitudinally contain the particles it was necessary to change the synchronous phase from -30^o to -37^o (the accelerating field was also increased to 1.66 MV/m to maintain the old acceleration rate). A change in synchronous phase is much more effective than an increase in accelerating field in maintaining a potential well in the presence of space charge. The results for the discrete gap calculation are shown in Figs. 2 and 3. There were 150 gaps in this simulation. Phase damping was not decreased by making the longitudinal forces discrete. The transverse emittances increased by about 15% (this may be partly numerical). The longitudinal emittance containing 90% of the particles increased by about a factor of two. This growth is filamentation caused by the nonlinear external longitudinal potential. Such an increase can be reduced by matching to the actual nonlinear potential (the initial distribution was matched to the harmonic restoring potential).

Conclusions

Most calculations were done assuming harmonic oscillator focusing forces and continuous acceleration. We found that even a beam near the space-charge limit was well behaved. Phase damping is still present and emittance growth because of mismatches is not noticeable. Nonlinearities and couplings introduced solely by space charge apparently have little effect. But even in this model, we found that mismatches are undesirable because they produce growth in beam spatial dimensions.

With discrete longitudinal forces we found no degradation of phase damping compared to the continuous case. Space-charge limited beams will probably have to be contained by using larger magnitudes of synchronous phases. Longitudinal emittance growth was

*I thank M. Weiss for pointing out the importance of this effect.

observed owing to filamentation caused by the large external nonlinearity.

These calculations indicate that future studies should look at the effects of external nonlinearities and couplings in space-charge limited beams. Also, other types of mismatches (other kinds of initial distributions) should be studied. Nonaxisymmetric features such as quadrupole magnets may change some conclusions but a proper study of these features will require three-dimensional space-charge calculations.

Acknowledgments

I thank R. Jameson for useful discussions and also S. Cheng for assistance with the numerical work.

References

1. W. P. Lysenko, "Equilibrium Phase-Space Distributions and Space Charge Limits in Linacs," Los Alamos Scientific Laboratory report LA-7010-MS (October 1977).
2. R.L. Gluckstern, R. Chasman, and K. Crandall. Proc. 1970 Proton Linear Accelerator Conf., National Accelerator Laboratory, 1970, p. 823.
3. R. Chasman, Proc. 1968 Proton Linear Accelerator Conf., Brookhaven National Laboratory, 1968, p. 372.

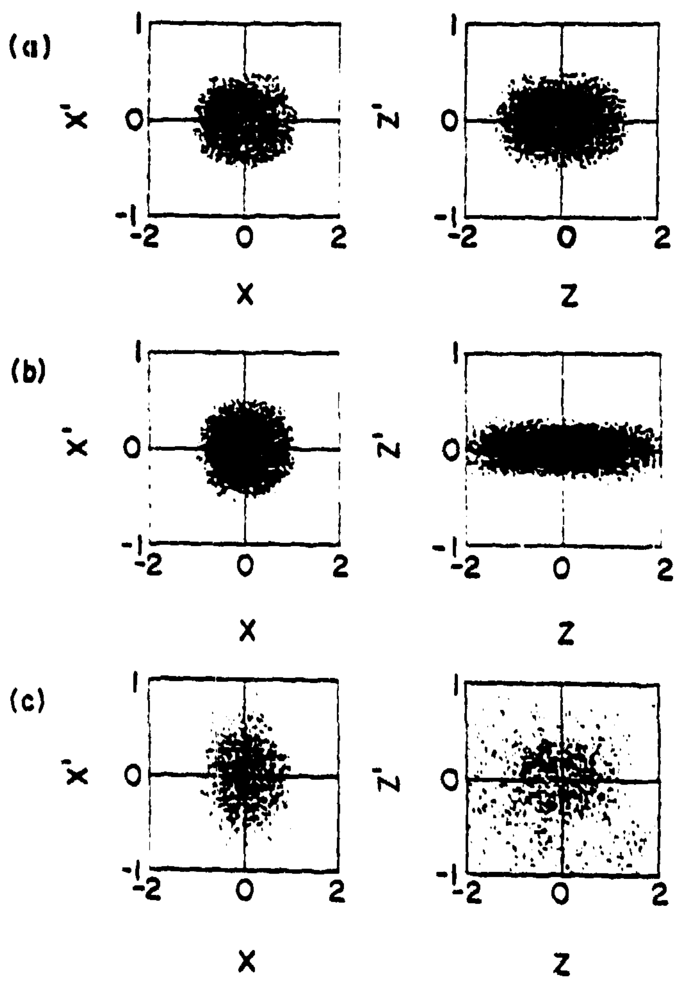

Fig. 2. The transverse and longitudinal phase-space projections are shown for the initial distribution (a), the final distribution for the continuous acceleration and harmonic focusing case (b), and the final distribution for the discrete gap forces case (c). Units are mm for x and z and mm-mrad for $x' = dx/dct$ and $z' = dz/dct$.

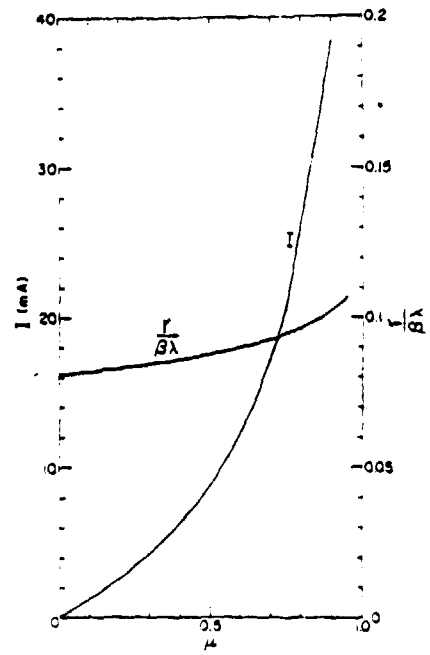

Fig. 1. The current and beam radius for equilibrium distributions with $\alpha = 0.67$ and $n = 2$ are shown as a function of the space-charge parameter μ. The transverse emittance value and all accelerator parameters are fixed.

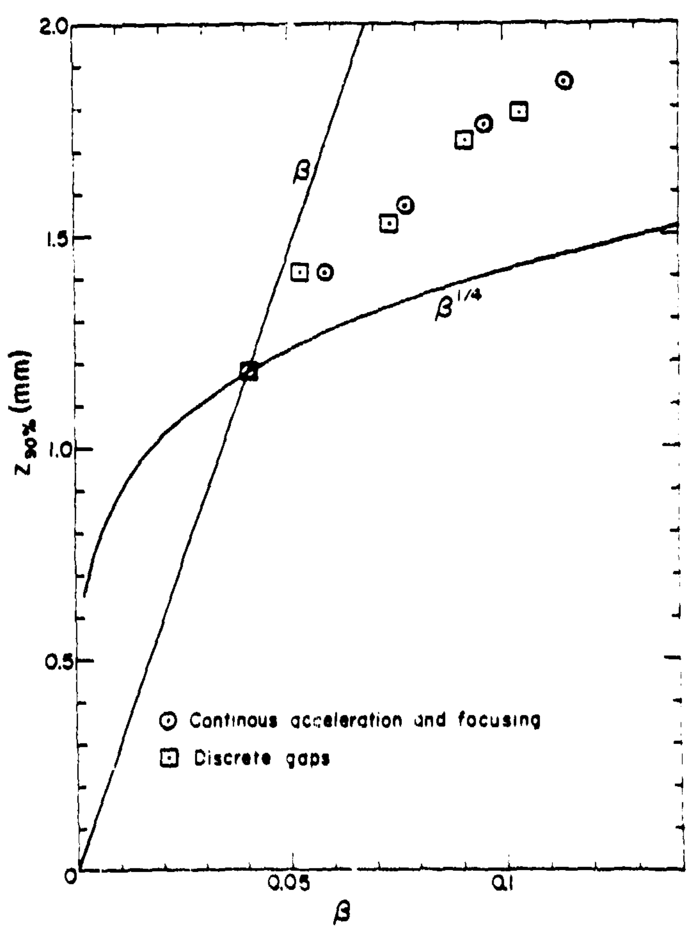

Fig. 3. The bunch length is shown as a function of β for both the continuous acceleration and discrete gaps cases.